Self-regulated production of an automotive composite floor pan

Michael Emonts, Kai Fischer, Sebastian Stender, Nadine Magura

Aachen Center for Integrative Lightweight Production (AZL) of RWTH Aachen University
Campus Boulevard 30, Bauteil 1A
Aachen, NRW/Germany

Institute for Plastics Processing (IKV) at RWTH Aachen University
Seffenter Weg 201
Aachen, NRW/Germany

ABSTRACT

In collaboration with seven partners from industry, the Aachen Center for Integrative Lightweight Production (AZL) of RWTH Aachen University and the Institute for Plastics Processing (IKV) at RWTH Aachen University are developing a self-regulating production system for structural composite parts, which combines the automated preforming technologies 3D Fiber Spraying and Towpreg Placement with a High Pressure Resin Transfer Moulding (HP-RTM) process. By embedding optical measuring equipment and a structural simulation into the production system, the system itself is capable to detect production fluctuations of the 3D Fiber Spraying process and to compensate these by deliberately adjusting the fiber structure of the subsequent Towpreg Placement process. The technical and economic advancement of this self-regulating system is demonstrated by the manufacturing of an automotive floor pan from long and continuous fiber reinforced epoxy.

In this paper, the impact of production fluctuations on the mechanical performance is shown for representative load cases. Subsequently, the effect of a deliberate adjustment of the continuous fiber structure on the component stiffness is numerically investigated. Laws for fluctuation compensation are derived and presented.

1. INTRODUCTION

The High Pressure Resin Transfer Molding (HP-RTM) process is one of the suitable processes to produce fiber-reinforced plastics for medium and large volume automotive series [1, 2]. Typically, the process sequence of the HP-RTM process for the production of thermoset components consists of the steps preforming and resin injection [3]. Preforming, in turn, is divided into the steps of cutting single reinforcing fiber layers from semi-finished textile products, stacking the fiber layers according to load requirements, heating and forming of the stack and trimming the shaped preform. Complex components, such as the automotive floor pan presented in this study, can also consist of several sub-preforms, so that these steps are carried out for each sub-preform. Before the HP-RTM step, the individual sub-preforms are usually assembled manually and inserted into the HP-RTM tool. In the HP-RTM process, resin, curing and release agent are mixed in a high-pressure mixing head, injected into the mold to impregnate the reinforcing fibers, and cured under pressure and temperature.

Copyright 2019. Used by the Society of the Advancement of Material and Process Engineering with permission.

SAMPE Conference Proceedings. Charlotte, NC, May 20-23, 2019. Society for the Advancement of Material and Process Engineering – North America.

Due to the complex shape of the floor pan (flank angle >80 °, multiple biaxial curvature) and thus three sub-preforming steps, approximately 6 kg from initial 13 kg textile fabrics are scrapped during preforming. With the goal to reduce the scrap rate to below 5 % and by this reducing production costs of the floor pan by 50 %, the AZL, IKV and seven partners from industry have merged the preforming technologies 3D Fiber Spraying and Continuous Towpreg Placement in one production system with a HP-RTM process.

In 3D Fiber Spraying, fiber rovings are used directly instead of semi-finished textile products. These rovings are fed to a robot-guided cutting unit, cut to the desired length (maximum 100 mm), oriented via a guiding unit (maximum anisotropy ratio of the bending strength in 0 ° and 90 ° direction of 1:3) and sprayed almost in net-shape onto a three-dimensional depositing tool [4]. In order to achieve the mechanical performance of a textile based floor pan, the long glass fiber preform is reinforced with a grid of continuous carbon fiber towpregs on top and bottom surface.

Disadvantageous to the 3D Fiber Spraying process is that fluctuations in the fiber areal weight (approximately 10 %, [5]) and fiber orientation can occur. Besides the obvious effect on the mechanical performance, fluctuations in the fiber architecture affect the flowing behavior of the resin mixture [6] and may even inhibit complete impregnation.

In order to autonomously compensate the fluctuations of the 3D Fiber Spraying process by adjusted towpreg grid design and to secure complete impregnation of the individual preform, predictive quality control is integrated into the production system (research project “iComposite 4.0"; funded by the German Federal Ministry of Education and Research (BMBF)).

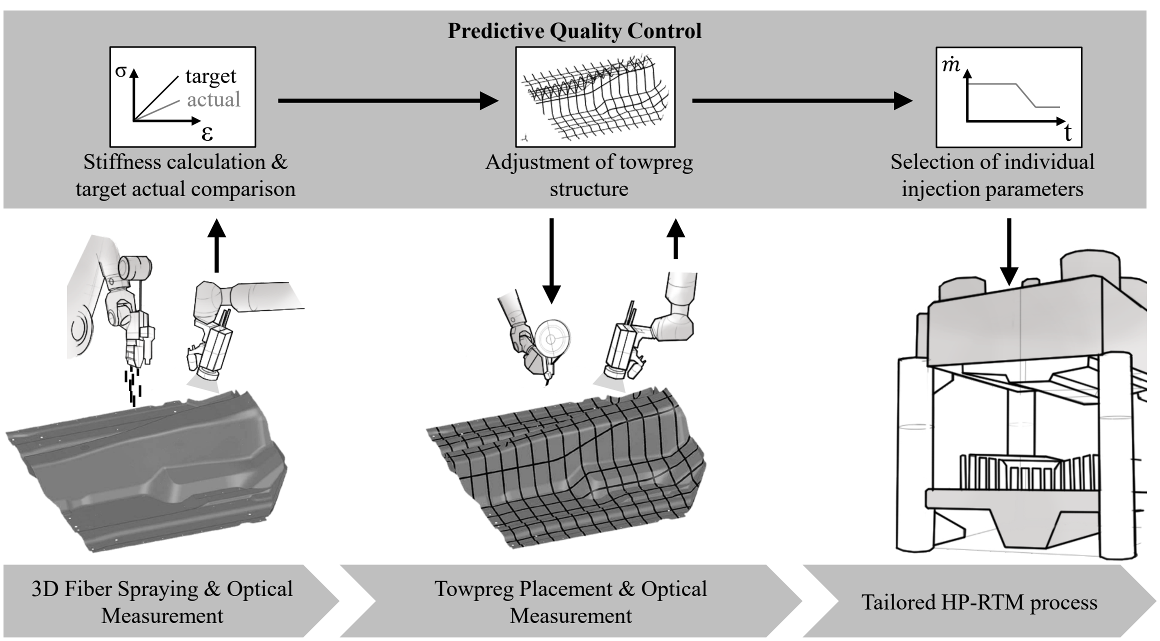

Figure 1. Principle of the self-controlled production system

Figure 1 depicts the self-controlled production system. Subsequent to the 3D Fiber Spraying process, an optical measuring system is used to determine the local fiber areal weight and fiber orientation of the preform. Structural simulation is used to calculate the actual component stiffness based on the measurement data. An algorithm is used to compare the actual stiffness with a target value. In case the actual value is below the target value, the fiber structure of the standard towpreg design is autonomously adjusted in the subsequent Towpreg Placement process to compensate for the lack of component stiffness. In a second step, individual impregnation parameters are selected to secure complete impregnation of the individual preform with fast curing epoxy in the subsequent HP-RTM process.

In addition to AZL (system integration and handling automation) and IKV (3D Fiber Spraying and material testing), the companies Apodius GmbH, Aachen (optical measuring system), BA-Composites GmbH, Grenzach-Wyhlen (Continuous Towpreg Placement machine), Frimo Sontra GmbH, Sontra (RTM mold), Frimo Lotte GmbH, Lotte (injection machine), ID-Systec GmbH, Neumünster (RFID label), Schuler Pressen GmbH, Göppingen (deliberate mold deflection control), Siemens AG, Munich (draping simulation and process automation), and Teijin Carbon Europe GmbH, Wuppertal (design, predictive control) are involved in the project.

2. METHODICAL APPROACH

The demonstrator component within the iComposite 4.0 project is a non-commercial automotive floor pan. As no detailed specification sheet for the floor pan exists, a variety of typical load cases is initially researched and three general load cases are selected. Subsequently, the exact amount of force, point of application of force and boundary conditions are determined under the constraint of deformation within linear-elastic material behavior. Since the geometrical complexity of the floor pan inhibits fundamental investigations of the stiffness compensation algorithm, a planar test geometry is introduced and the load cases are transferred to this test geometry (Section 3).

Next, a numerical study on the qualitative effects of towpreg position and placement angle on the overall stiffness of the test geometry is conducted for the three load cases torsion, bending and compression (Section 4). Based on these results, a qualitative study on the effect of the towpreg position on the overall stiffness is conducted and the laws for the stiffness compensation algorithm are derived (Section 5).

Thereafter, the capability of the stiffness compensation algorithm is numerically demonstrated for the test geometry (Section 6).

3. REPRESENTATIVE LOAD CASES AND MODEL DESIGN

Both, driving performance as well as passenger safety are highly defined by the global stiffness of the body of a passenger car. Torsional stiffness and bending stiffness, in turn, are two main parameters to evaluate global stiffness and thus are used to investigate innovative body concepts in a large number of studies [for example 7, 8, 10, 11]. Torsion of the body of a passenger car results, for instance, from centrifugal forces when driving through curves with elevated velocity or from an unbalanced load distribution when driving onto a curbstone. Bending of the body occurs, for example, from acceleration of the car or the weight of passengers and car interior. Both, torsional stiffness and bending stiffness are significantly influenced by the stiffness of the floor pan [7] and thus are selected for the research of this study.

In addition, as part of the passenger compartment, the floor pan is highly relevant for passenger safety [10]. Therefore, besides the global stiffness load cases, front crash is also considered for this study.

In order to evaluate the compensation of fluctuations of the mechanical properties, these load cases are simplified and applied to a model of the floor pan. The boundary conditions for the simulation, in particular fixing constraints and load introduction, are adapted from different studies [for example 7, 9, 10, 11] as depicted in Figure 2.

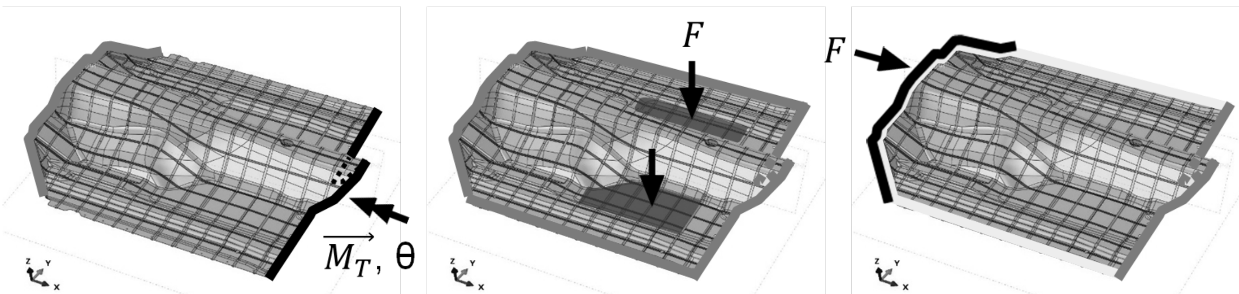

Figure 2. Model design for the numerical investigations: torsion stiffness (left), bending stiffness (middle) and in-plane stiffness (right)

For investigations on the torsion stiffness K_T, all degrees of freedom (DOFs) of the edge of the left side are set to zero whilst a rigid clamp is tied to the edge of the right side to introduce torsion around the x-axis. The maximum torsion angle θ of the body in white derived from literature was 0.3 ° [10]. As an assessment to the safe side, in the present study a torsion angle θ of 1 ° is used.

For the investigations on the bending stiffness K_B, bending due to the weight of front seats and front passengers is simulated. The 95 % percentile weight of a male adult in Germany is 100 kg [12] and the weight of a passenger seat is assumed to be 20 kg. Thus, at the location of both front seats, an area force of 0.0141 MPA (equivalent the weight of 120 kg) in negative z-axis direction is applied. For the simulation all DOFs of the floor pan edges are set to zero.

The sensible conversion of the boundary conditions of the highly dynamic front crash of a full vehicle to static compression stiffness of the floor pan is the most challenging one. For this load case all DOFs of the edge of the right side of the floor pan are set to zero, whilst a rigid clamp is tied to the edge of the left side. A compression force is applied to the clamp and displacement of all edges is limited to the x-axis direction. The compression force is increased until a maximum stress of 20 % of the compression strengths of the fiber sprayed material occurs to secure investigations within linear-elastic material behavior. Following this routine, a compression force of 25 kN is determined.

In addition, for fundamental investigations on the stiffness compensation algorithm, a planar test geometry is used (Figure 3).

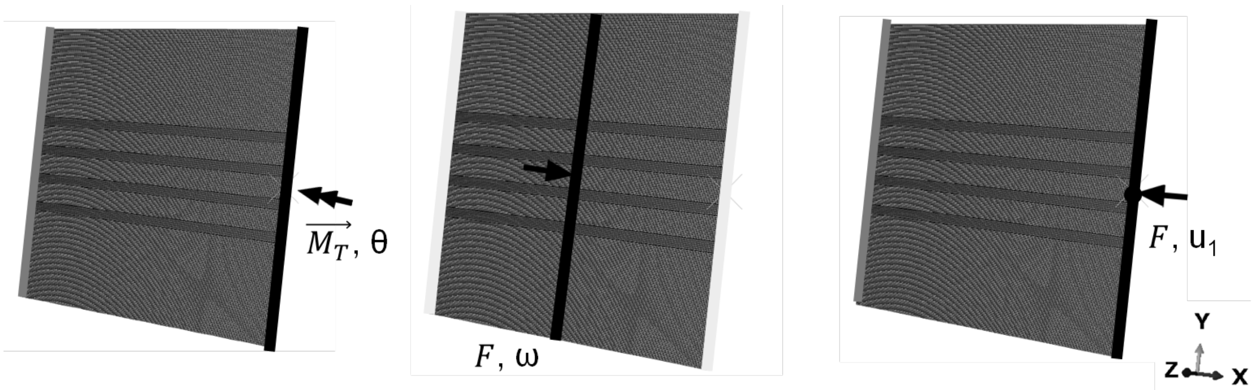

Figure 3. Model design for the test geometry: torsion stiffness (left), bending stiffness (middle) and compression stiffness (right)

Since experimental validation of the compensation is planned, the dimensions of the test geometry for numerical investigations are limited by the maximum dimension of the available RTM equipment and thus are set to 400 * 400 mm².

For investigations on the torsion stiffness K_T, all degrees of freedom (DOFs) of the left side edge of the test geometry are set to zero, whilst for the right side edge only displacement in and rotation around the x-axis direction are allowed. A rigid clamp is tied to the right side edge to introduce torsion around the x-axis. In order to minimize artifacts caused by a takeup of slack and alignment or seating of the specimen during experimental testing, the torsion angle θ is increased to 10 °. With given torsion angle θ and measured resulting torsion momentum M_T the torsion stiffness K_T is calculated according to Eq. 1 [7]:

$$K_T = \frac{M_T}{\theta} \qquad \text{[Eq. 1]}$$

The boundary conditions of the numerical investigations of the bending stiffness are derived from the testing norm DIN EN ISO 14125 [13]. Replacing the supports, displacement in x-axis direction and rotation around the y-axis are allowed for the left and right edge of the test plate. All other DOFs are prohibited. In the center between both edges, a rigid body is modelled, representing the load nose. The maximum displacement in z-axis direction from the investigations on the floor pan model is applied to the load nose, which is 10 mm. With given displacement w, support span L and measured reaction force F_B the bending stiffness K_B is calculated according to Eq. 2 [13]:

$$K_B = E * I = \frac{F_B * L^3}{48w} \qquad \text{[Eq. 2]}$$

The test setup for the investigation of the compression stiffness K_C is modelled in good agreement to DIN EN ISO 14126 [14]. All DOFs of the left side edge of the test geometry are prohibited. A rigid clamp is tied to the right side edge to introduce the compression force F_C. For the clamp, only displacement u_1 in x-axis direction is allowed. K_C is calculated following Eq.3, where L_0 is the initial specimen length:

$$K_C = E * A = \frac{F_C * L_0}{u_1} \quad \text{[Eq. 3]}$$

4. QUALITATIVE STUDY ON THE EFFECT OF TOWPREG POSITION AND PLACEMENT ANGLE ON THE COMPONENT STIFFNESS

A lack of component stiffness due to production fluctuations during the 3D Fiber Spraying process can be compensated with various adjustments of the reinforcing towpreg grid. For the selection of the optimum design, several aspects, such as material efficiency, effects on producibility, residual stresses and sensitivity of the compensation, must be taken into account. In order to identify the most sensitive parameters of the towpreg grid, a qualitative study of the effect of towpreg position and placement angle β on the component stiffness is conducted.

For this qualitative study the test geometry is used. Four carbon fiber towpreg strips (each with a thickness of 0.25 mm, width 11.5 mm, E_1 = 123.8 GPa and E_2 = 7.4 GPa) are tied to the base plate from long glass fiber reinforced epoxy (thickness = 2 mm, E = 20 GPa, isotropic) (Fig. 4). The spacing between two towpreg strips and the placement angle β are varied as described in Table 1.

Table 1. Variation parameters of the qualitative study

Label	Description	Variation	Position index 0	Position index 1
Design 1: Spacing in Y	4 towpregs are oriented parallel to the x-axis direction	Spacing in y-axis direction is varied in 11 steps from 0 mm to 118 mm	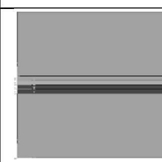	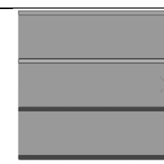
Design 2: Spacing in X	4 towpregs are oriented parallel to the y-axis direction	Spacing in x-axis direction is varied in 11 steps from 0 mm to 118 mm		
Design 3: Spacing in Y and X	2 towpregs are oriented parallel to the x and 2 towpregs parallel to the y-axis direction	Spacing in x- and y-axis direction is varied in 11 steps from 0 mm to 377 mm	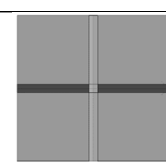	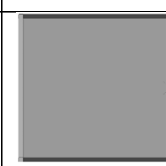
Design 4: Angle, one-sided	2 towpregs are oriented parallel to the x and 2 towpregs parallel to the y-axis direction	Placing angle β is varied in 16 steps from 0 ° to 45 °	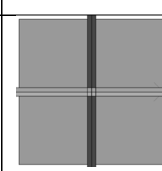	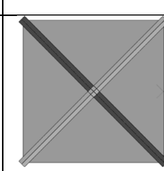

Design 5: Angle, on both sides	On both sides of the bas plate 1 towpreg is oriented parallel to the x and 1 towpreg parallel to the y-axis direction	Placing angle β is varied in 16 steps from 0 ° to 45 °	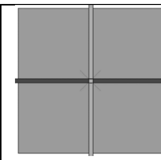	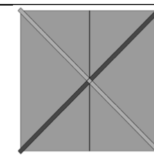

The sensitivity of the torsion stiffness to towpreg position and placing angle is shown in Figure 4.

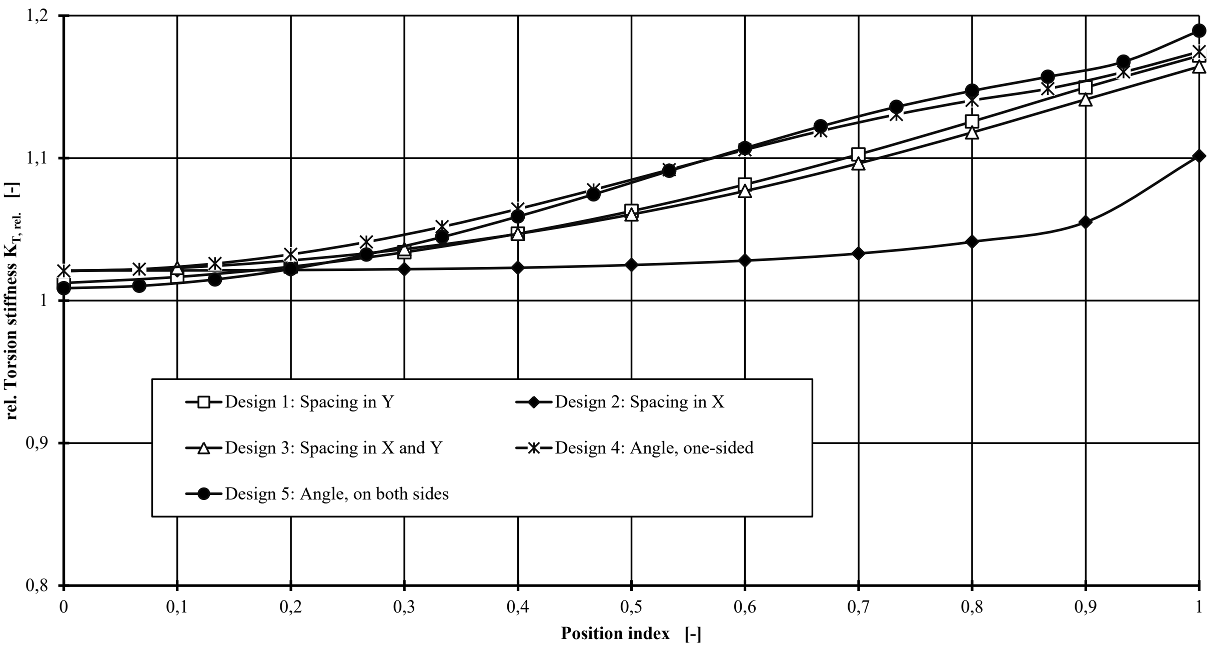

Figure 4. Influence of towpreg position and placing angle to the torsion stiffness

In order to enable direct comparison between the influences on torsion, bending and compression stiffness, the stiffness values K_i are normalized by the stiffness of the long glass fiber reinforced base plate $K_{i,\,GFRP}$, Eq. 4:

$$K_{i,rel.} = \frac{K_i}{K_{\mathrm{i,GFRP}}} \qquad \text{[Eq. 4]}$$

It can be derived from Figure 5 that all designs initially increase torsion stiffness by approximately 2 %. The placing angle has the most dominant influence on the torsion stiffness as the fiber axis is shifted towards 45 °, which is favorable for shear loads. No significant difference between one-sided and two-sided reinforcement can be observed. At 45 °, the torsion stiffness is increased by 17.5 % and 19 % respectively.

Besides the placement angle, the spacing in y-axis direction significantly influences the torsional stiffness, as the towpregs are shifted towards the locations of highest deflection. At the maximum spacing, the torsion stiffness is increased by 17% (Design 1) and 16 % (Design 3). When the towpregs are shifted towards the fixing and the clamp edge, torsion stiffness increases only moderately. Only starting from position index 0.7, the increase in torsion stiffness becomes more obvious. At positioning index 1, the improvement of torsion stiffness reaches 10 %.

Figure 5 depicts the influence of towpreg position and placing angle on the bending stiffness of the test geometry. When all four towpregs are oriented perpendicular to the load nose, the bending stiffness is initially increased by 26 %. A variation of the spacing between the towpregs only has minor effect on the bending stiffness; the maximum increase is 28.5 % at position index 1, which is the maximum stiffness among all designs.

For small position indexes, the designs 3, 4 and 5 are fairly similar and therefore have similar increase on the bending stiffness of approximately 16 %. As the spacing between the towpregs placed parallel to the load nose increases for Design 3, the bending stiffness slightly decreases, reaching a value of 1.14 for position index 1. An increasing placement angle results in a decreasing Young´s modulus of the towpregs in direction of the bending. Thus, with increasing placement angle, the bending stiffness decreases constantly, reaching values of 1.13 (Design 4) and 1.1 (Design 5).

When all towpregs are oriented parallel to the load nose, the bending stiffness is increased by 21.5 % at position index 0. By varying the spacing between the towpregs, and thereby increasing the distance to the area of load introduction, the bending stiffness declines constantly. The minimum stiffness of 1.06 is reached at position index 1, which is the minimum stiffness among all designs. The bending stiffness is most sensitive to variations of the position of towpregs placed parallel to the load nose.

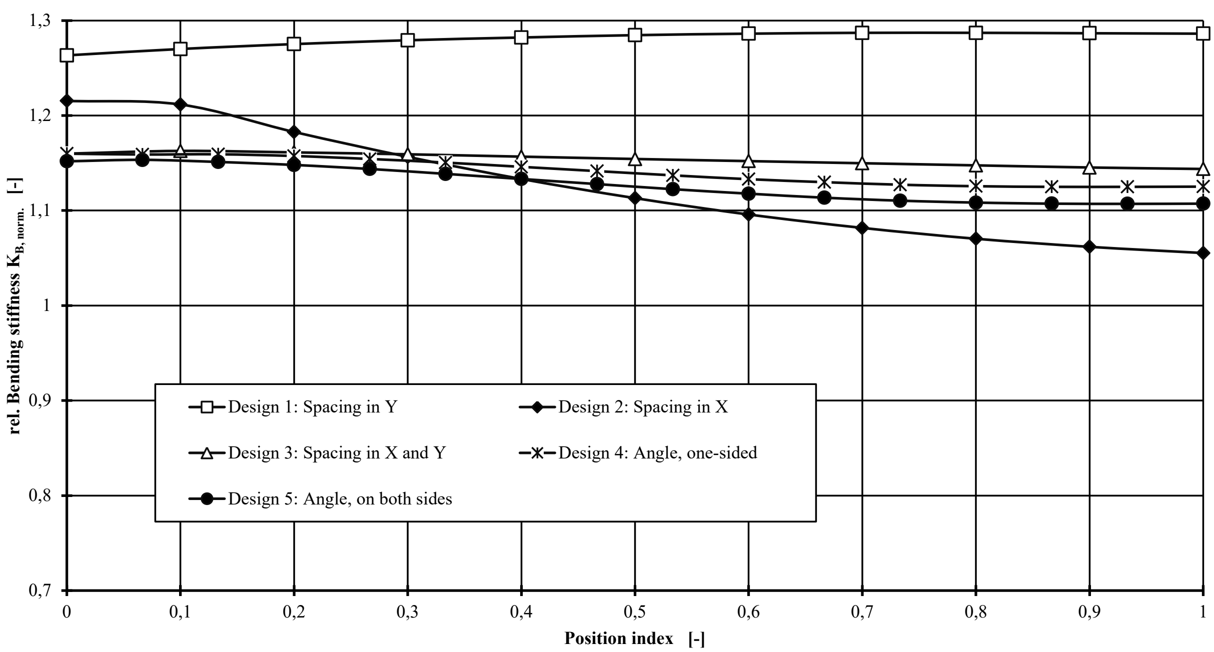

Figure 5. Influence of towpreg position and placing angle to the bending stiffness

In Figure 6 the influence of towpreg position and placing angle on the compression stiffness is shown. All designs result in an increase in bending stiffness. It can be seen that the spacing between the towpregs does not affect the bending stiffness (Designs 1, 2 and 3) and that an orientation of all towpregs parallel to the compression load (Design 1) is the most favorable design to increase compression stiffness. For Design 1 the maximum increase in compression stiffness is 8.5 %. An orientation of the towpregs parallel to the load nose adds least to bending stiffness (5.5 %).

As for bending stiffness, an increase in placement angle reduced the Young´s modulus of the towpregs in the load bearing direction and therefore reduces the compression stiffness.

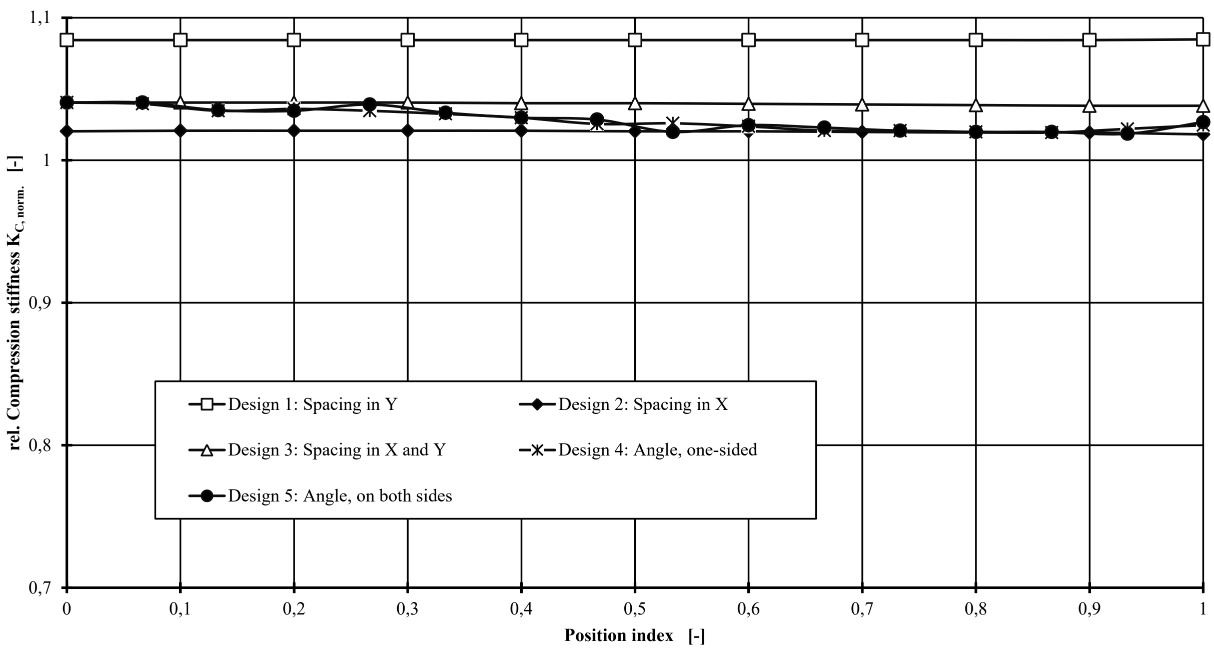

Figure 6. Influence of towpreg position and placing angle to the compression stiffness

The compensation of production fluctuations of the 3D Fiber Spraying process through individual towpreg grids has to be both, material efficient and sensitive regarding the resulting stiffness. Therefore, a design must be chosen, for which one additional towpreg increases the most torsion, bending and compression stiffness, yet allowing for sensitive adjustments to reach the target stiffnesses as precisely as possible. Furthermore, producibility and drapability of the grid design must be considered, taking the complex geometry of the floor pan into account. Therefore, only one design for compensation is chosen.

Torsion stiffness is most sensitive to adjustments of the placing angle. At a maximum β of 45 ° the torsion stiffness is increased by 19 %. However, in order to cover the complete dimension of the base plate, the initial length of the towpreg strips has to be increased by approximately 41 %. Thus, material efficiency is reduced. In addition, in contrast to torsion load, for bending and compression a deviation from $\beta = 0$ ° has a negative effect on the stiffness.

Placing all towpregs in y-axis direction has a minor effect on torsion stiffness. Furthermore, torsion stiffness is least sensitive to increasing spacing between the towpregs. For bending stiffness, reinforcements placed directly at the load nose in y- axis direction increase bending stiffness by 21.5 %. Additionally, bending stiffness is most sensitive to the spacing between the towpregs. However, in contrast to torsion stiffness, an increased spacing results in a decreasing bending stiffness. Design 2 also has the least reinforcing effect on compression stiffness with no obvious sensitivity to the spacing.

When all four towpregs are placed in x-axis direction, torsion stiffness is nearly as sensitive to the spacing as to an increasing placement angle. The maximum torsion stiffness reached is 1.17. Bending stiffness and compression stiffness do not significantly change with the towpreg spacing for Design 1. However, placing all four towpregs in x-axis direction increases both values the most.

While torsion stiffness is fairly sensitive to Design 3, adjustments of the spacing in x and y-axis direction do not influence compression stiffness and have a minor negative effect on bending stiffness.

Due to the significant influence of the towpreg position as well as the positive reinforcing effect on all three load cases, Design 1 is chosen for the stiffness compensation algorithm.

5. QUANTITATIVE STUDY ON THE EFFECT OF THE TOWPREG POSITION ON THE COMPONENT STIFFNESS

The stiffness compensation algorithm will be implemented into the production system. Despite the limitation to placing compensation towpregs parallel to x-axis direction, numerical simulation of all possible combinations of number of towpregs and towpreg positions within the production does not seem efficient. Therefore, a simple algorithm is developed, which is based on the fact that the increase in stiffness resulting from a combination of towpregs is equal to the sum of the increases in stiffness resulting from each individual towpreg. This is in particular true for symmetrical designs [15].

For the development of the stiffness compensation algorithm, the following assumptions are made:

- The algorithm can only add towpregs to the standard towpreg design
- The towpreg position can only vary in 11.5 mm steps, as this is the lane width of the placement head
- No overlay between towpregs is allowed, as this is expected to prevent impregnation of the underlying long fibers
- The laminate must be symmetrical in width and thickness direction to avoid warpage due to residual stresses. Therefore, every position contains a set of four towpregs.

When these assumptions are applied to a test geometry with standard towpreg design and 400 mm edge length, 15 possible towpreg positions remain (Figure 7).

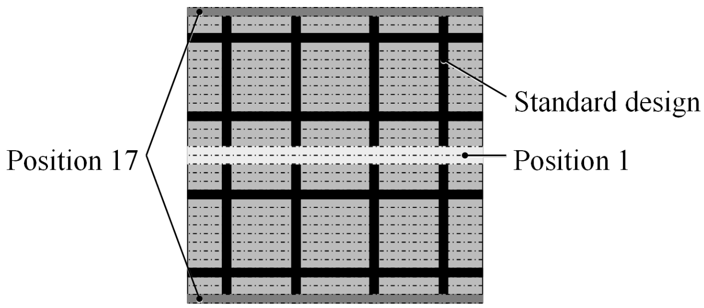

Figure 7. Towpreg positions available for compensation

In order to calibrate the stiffness compensation algorithm, a numerical study is conducted, quantifying the increase in stiffness $\Delta K_{i,j}$ of the test plate with standard design resulting from a set of four extra towpregs at position j. The results of the study on torsion stiffness are depicted in Figure 8.

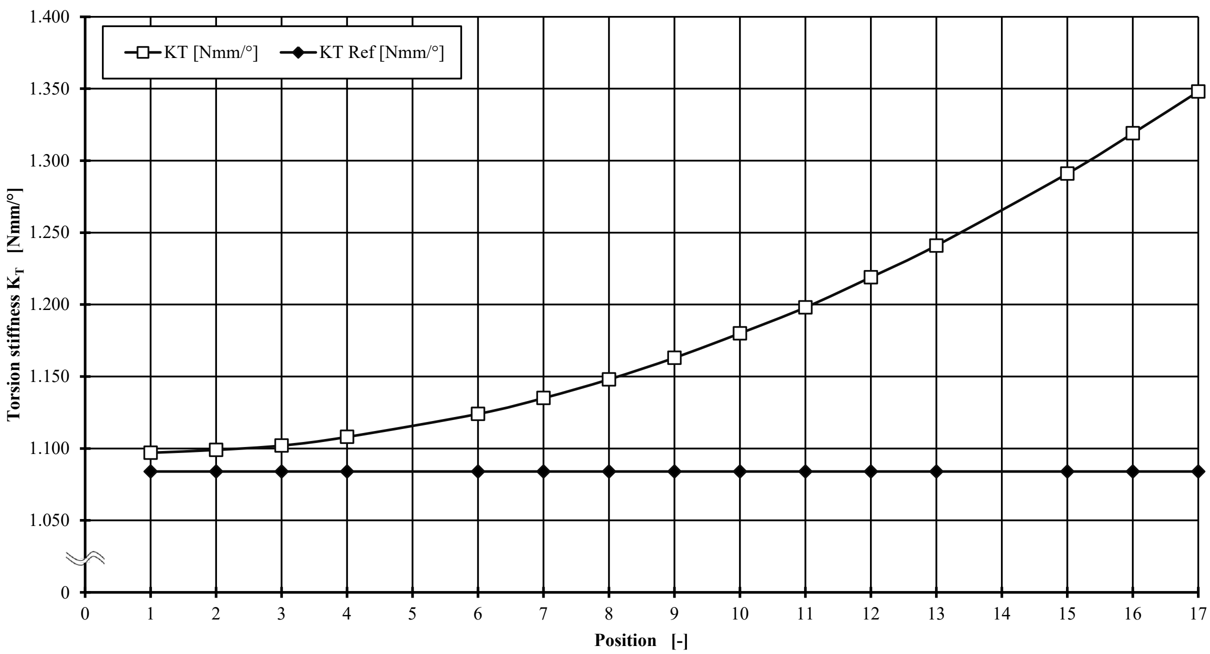

Figure 8. Increase in torsion stiffness $\Delta K_{T,j}$ per towpreg position j

It can be seen that when the four towpregs are placed in the middle of the test plate (Position 1), the torsion stiffness of the standard design is increased by 11.5 Nmm/°. When the four towpregs are placed further to the outside edges, the stiffness increase grows steadily until the maximum value 241 Nmm/° at Position 17 is reached. At Positions 5 and 14 the towpregs of the standard design are placed. Therefore, no additional towpregs can be placed at these positions.

As the influence of the position of the extra towpregs is negligible for bending and compression, the increase in stiffness per set can be approximated as $\Delta K_B = 1.83$ Nm² and $\Delta K_C = 1{,}448.2$ kN.

With these values, the number of required sets for compensation n can be calculated for the three load cases following Eq. 5 and 6:

$$n_i = \frac{K_{i,target} - K_{i,actual}}{\Delta K_\mathrm{i}} \quad \text{[Eq. 5]}$$

$$n = \max(n_i) \quad \text{[Eq. 6]}$$

As the stiffness increase per extra towpreg for torsion is fairly large compared to the compression load case (Figures 5 and 7), ΔK_T can be approximated with the maximum value 241 Nmm within this calculation.

Finally, the combination of extra towpreg sets, which enables the most precise compensation of production fluctuations, can be selected.

6. NUMERICAL VALIDATION OF THE STIFFNESS COMPENSATION ALGORITHM

To validate the compensation algorithm, the Young´s modulus of the base plate is reduced in four steps from 20 GPa to 12 GPa. Subsequently the resulting stiffnesses are simulated for the three load cases and the algorithm is executed.

The results of the validation are presented in Table 2:

Table 2. Results of the numerical validation

Young´s modulus [GPA]	20 (reference)	18	16	14	12
$K_{T,\ actual}$ [Nmm/°]	1084	1000	916	831,8	747,5
n_T	-	1	1	2	2
$K_{B,\ actual}$ [Nm²]	11.65	10.9	10.2	9.5	8.8
n_B	-	1	1	2	2
$K_{C,\ actual}$ [kN]	20,768.5	19,002.4	17,234	15,468	13,698.6
n_C	-	2	3	4	5
n	-	2	3	4	5
Towpreg position	-	1, 9	1, 6, 12	1, 2, 3, 16	1, 2, 4, 7, 17
$K_{T,\ res.}$ [Nmm/°]	1084	1092	1104	1112	1115

$K_{B,\,res.}$ [Nm²]	11.65	15.2	16.6	17.9	19.3
$K_{C,\,res.}$ [kN]	20,768.5	21,857.9	21,516.9	21,175.2	20,844.2

It can be derived from Table 2 that the production deviations have significant influence on the mechanical performance for all load cases. The biggest effect on stiffness can be observed for the compression load case.

For all deviations and load cases, after application of the stiffness compensation algorithm, the resulting stiffnesses exceed the target values. Furthermore, in particular for compression and torsion load case, the target values are reached with good precision, leaving a maximum deviation of 2.9 % for torsion and 5 % for compression. However, the deviations for bending stiffness are fairly large, with a maximum deviation of 65 % for fiber volume content 30 %. This results from the fact that one extra towpreg contributes relatively little to compression stiffness. As a consequence, the number of towpreg sets required for compensation for this load case n_C is fairly high compared to bending and torsion and thereby determines the number of towpreg sets used for compensation n. Unlike for torsion, the stiffness contribution of one extra towpreg cannot be adjusted by position for bending, resulting in the large exceed of the target bending stiffness.

7. CONCLUSIONS & OUTLOOK

The combination of 3D Fiber Spraying and Towpreg Placement is highly capable for the production of cost-sensitive FRP components. However, process induced deviations of the 3D Fiber Spraying process influence the mechanical performance of the upcoming part.

Therefore, a predictive quality control is integrated into a production system with 3D Fiber Spraying, Towpreg Placement and HP-RTM. Part of the quality control is an algorithm, which is capable for the identification of towpreg structures for stiffness compensation.

In this paper, the emergence of this algorithm is described. For three representative load cases, it is shown that placing extra towpregs in load direction of the torsion momentum and compression force and perpendicular to the bending load nose offers both, the most efficient stiffness increase as well as the best option to precisely adjust the amount of stiffness added.

Furthermore, it is shown, that extra towpregs for the compensations of reduced bending stiffness should be at the location of or closed by to the location of load introduction.

Finally, the stiffness compensation algorithm was demonstrated for a test geometry for four different production deviation scenarios. For all scenarios and all load cases, by adjusting the towpreg grid, target values is reached. Furthermore, for compression and torsion precise control of the stiffness is demonstrated.

In the future, the algorithm will be integrated into the production environment and validated practically. Manufacturing influences, such as precision of the placement of the reinforcing towpregs, residual stresses due to the material combination and thickness variations due to the varying preform design will be investigated.

This research and development project is funded by the German Federal Ministry of Education and Research (BMBF) within the Framework Concept “Research for Tomorrow’s Production” (02P14A045) and managed by the Project Management Agency Karlsruhe (PTKA). We would like to express our gratitude to both. The authors are responsible for the contents of this publication.

GEFÖRDERT VOM

Bundesministerium für Bildung und Forschung

BETREUT VOM

PTKA Projektträger Karlsruhe
Karlsruher Institut für Technologie

8. REFERENCES

[1] Patel, Critesh. *Development of discontinuous fibre preforming processes*. Nottingham: University of Nottingham, 2014

[2] Magagnato, Dino. *Charakterisierung und Simulation der Formfüllung beim Resin Transfer Molding unter Berücksichtigung der lokalen Faserstruktur*. Karlsruhe: Karlsruher Institut für Technologie (KIT), 2016

[3] Chaudhari, Raman. *Characterization of high-pressure resin transfer molding process variants for manufacturing high performance composites*. Pfinztal: Fraunhofer-Institut für Chemische Technologie ICT, 2014 - ISBN: 978-3-8396-0669-8

[4] Fecher, Marc L.. *Analyse des 3D-Faserspritzverfahrens zur Fertigung komplexer und funktionsintegrierter RTM-Strukturbauteile*. Aachen: Institut für Kunststoffverarbeitung (IKV), 2017 - ISBN: 978-3-95886-161-9

[5] Hopmann, Christian, Egger, Peter, Beste, Christian, Magura, Nadine, Müller, Norbert, Stender, Sebastian, Fischer, Kai. „Conference Paper Ausschussfreie FVK-Bauteilherstellung durch Inline-Prozessregelung“. *29. Internationales Kolloquium Kunststofftechnik 2018*. Aachen, 02/28 – 03/01/2018. Institut für Kunststoffverarbeitung(IKV). Print book – ISBN 978-3-8440-5609-9

[6] Meier, Reinhold. *Über das Fließverhalten von Epoxidharzsystemen und vibrationsunterstützte Harzinfiltrationsprozesse*. München: TU München, 2017 - ISBN: 978-3-8439-3211-0

[7] Chen, Wei, Zuo, Wenjie. “Component sensitivity analysis of conceptual vehicle body for lightweight design under static and dynamic stiffness demands.” *Int. J. Vehicle Design* 66 (2011): 107–123. DOI: 10.1504/IJVD.2014.064546

[8] Boeman, Reymond G., Johnson, Nancy L. “Development of a cost competitive, composite intensive, body-in-white”. SAE International, 2002. DOI: 10.4271/2002-01-1905

[9] Helsen, Jan, Cremers, Luc, Mas, Peter, Sas, Paul. “Conference Paper Global static and dynamic car body stiffness based on a single experimental modal analysis test.” *International Conference on Noise and Vibrations Engineering including USD2010*. Leuven, 2010

[10] Ickert, Leif, Thomas, Dieter, Eckstein, Lutz, Tröster, Thomas. *Beitrag zum Fortschritt im Automobilleichtbau durch belastungsgerechte Gestaltung und innovative Lösungen für lokale Verstärkungen von Fahrzeugstrukturen in Mischbauweise*. Frankfurt/M, Berlin: VDA, 2012

[11] Faber, Jakob. *Beitrag zur konstruktiven Gestaltung offener, verrippter Profile aus Faser-Thermoplast-Verbunden mit lastpfadgerechten Verstärkungen*. Darmstadt: TU Darmstadt, 2016

[12] Jürgens, Hans W. *Erhebung anthropometrischer Maße zur Aktualisierung der DIN 33402 - Teil 2*. Dortmund/ Berlin/ Dresden: Wirtschaftsverlag NW, 2004

[13] DIN EN ISO 14125, „Faserverstärkte Kunststoffe – Bestimmung der Biegeeigenschaften". Beuth Verlag, 2011

[14] DIN EN ISO 14126, „Bestimmung der Druckeigenschaften in der Laminatebene". Beuth Verlag, 2000

[15] Klein, Bernd. *Leichtbau-Konstruktion*. Wiesbaden: Springer Vieweg, 2009